

UW-Madison.

SSEC Publication No.89.10.S1.

Engineering Center

University of Wisconsin-Madison

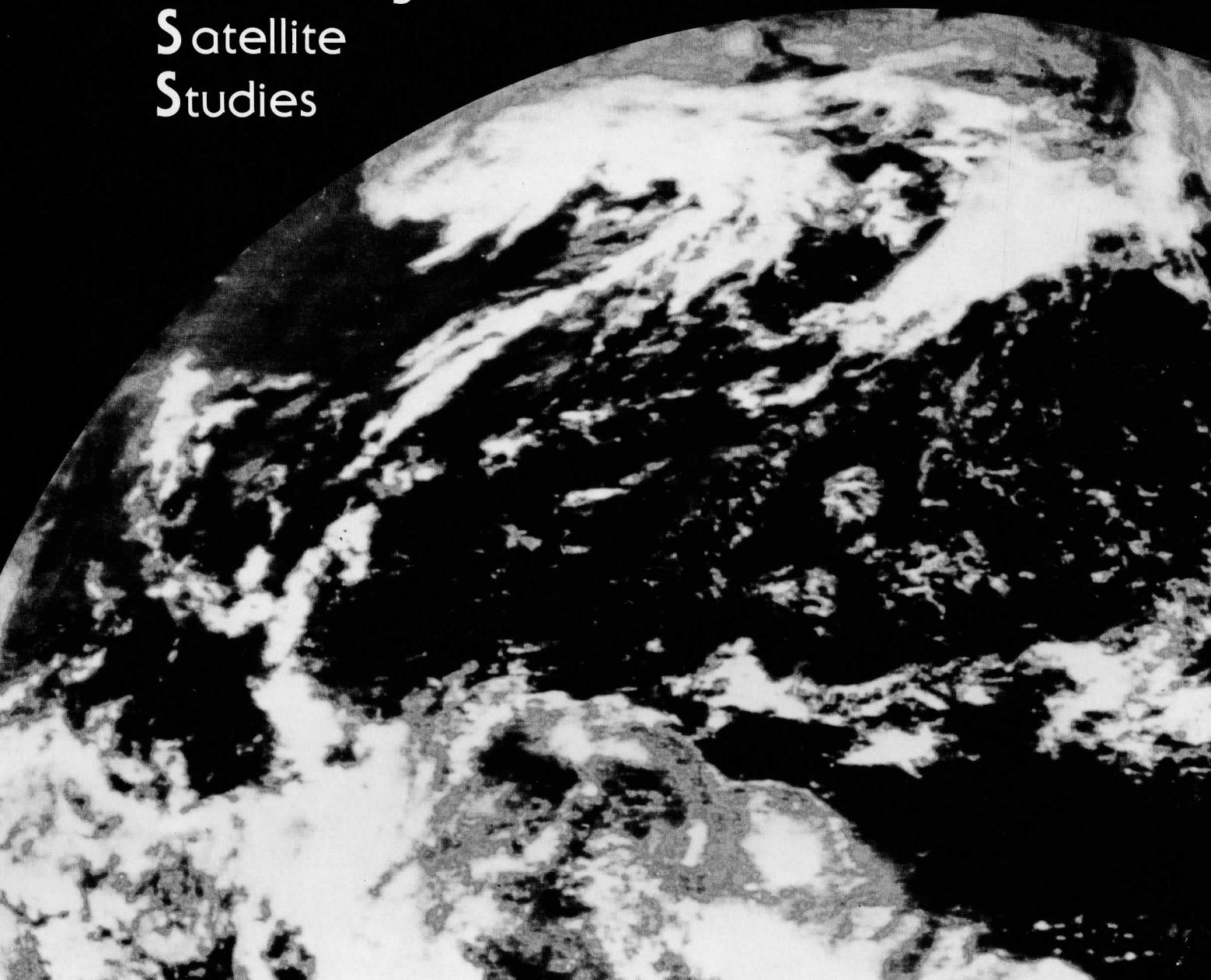
A Report to

The European Organisation for the
Exploitation of Meteorological Satellites (EUMETSAT)

25 W. Day
Madison, WI

A REPORT from the

Cooperative
Institute for
Meteorological
Satellite
Studies



The Schwerdtfeger Library
1225 W. Dayton Street
Madison, WI 53706

A Report to

The European Organisation for the
Exploitation of Meteorological Satellites (EUMETSAT)

for

Interim Report on Requirements for an Interferometer Sounder for Meteosat

Contract #: EUM/CO/89/15

for the period of

1 July 1989 to 30 January 1990

submitted by

William L. Smith
CIMSS Director

The Cooperative Institute for Meteorological Satellite Studies (CIMSS)

at the
University of Wisconsin-Madison
1225 West Dayton Street
Madison, Wisconsin 53706
608/263-4085

October 13, 1989

TABLE OF CONTENTS

I. Introduction.....1

II. General Assumptions and Objectives.....2

III. Results.....2

 A. Baseline Definition.....2

 B. Simulated Temperature and H₂O Sounding Performance.....5

 C. Operational Scenarios.....7

 D. Variations from the Baseline.....8

 E. Typical NEdT.....9

 F. Documentation of Calibration Requirements.....9

 G. Data Compression Techniques.....9

IV. Summary.....9

I. Introduction

This is an interim report of a study to define the requirements of an interferometer sounder for the next generation Meteosat. An interferometer sounder is required to produce high vertical resolution temperature and moisture soundings as needed for:

- (1) *Defining atmospheric stability tendencies as needed for forecasting local convection and subsequent weather.*
- (2) *Providing one to three hourly interval sounding data input to regional mesoscale analysis/forecast models.*
- (3) *Defining wind profiles for regional and global data assimilation systems through the animation of water vapor retrieved in eight narrow (1-2 Km) vertical layers.*
- (4) *Defining ocean and land surface skin temperature with high accuracy ($\sim 0.5^{\circ}\text{C}$) as needed for estimating surface heat fluxes.*
- (5) *Providing the pressure heights of clouds with high accuracy ($\sim 10\text{-}20$ mb), even for semi-transparent cirrus.*
- (6) *Observing stratospheric ozone patterns and lower tropospheric ozone concentration.*

The Michelson interferometer is the most efficient means of providing continuous spectra of earth-atmosphere radiance with relatively high spectral resolution. Simulations and experimental data from high altitude aircraft have demonstrated that soundings of atmospheric temperature and water vapor can be achieved with vertical resolutions and accuracies two to three times better than that currently achievable with filter radiometer instruments. This improvement is crucial for achieving the sounding accuracy needed to resolve stability features responsible for localized weather and for satellite soundings to be useful in numerical weather analysis/forecast models. Also, the relatively high spectral resolution of the radiometric data permits surface skin temperature and cloud pressure altitudes to be defined with much higher accuracies than are achievable with current sounding/imaging radiometers.

The unique advantage of implementing an interferometer sounder on a geostationary satellite is that both the local time tendency and the mass motion of the atmosphere can be observed. The tendency observation is important for local forecasting; the motion in as many as eight to ten distinct tropospheric layers provides wind soundings useful for input to global as well as regional data assimilation systems. Also, the use of the geostationary satellite optimizes the capability for observing the important near-surface temperature and water vapor features. This optimization occurs because one is able to observe at times when cloud obscuration is a minimum and when the surface background temperature possesses the greatest contrast with the overlying atmosphere.

The much higher information content provided by the quasi-continuous spectrum of outgoing radiance must be extracted from approximately two orders

of magnitude more spectral radiances than are provided by today's filter instruments. Fortunately, a new very efficient simultaneous parameters retrieval method has been developed to enable the processing to be accomplished at real-time rates even with today's medium-class computers. Tests of this highly efficient retrieval algorithm have been conducted with experimental aircraft data to demonstrate the achievement of the accuracy desired.

This interim report defines a conservative baseline specification for the next generation Meteosat. It is conservative in that all the requirements can be achieved with currently available hardware and the data can be handled with today's mid-class computers. The spectral and spatial resolutions are appropriate for achieving the desired meteorological products and accuracies at low risk to cost and performance. This preliminary report includes performance comparisons of the baseline interferometer system with a filter radiometer. The weight, power, and size requirements of the baseline Meteosat interferometer is comparable to that of a filter radiometer, even though the sounding performance is greatly improved.

II. General Assumptions and Objectives

The initial assumptions and tradeoff considerations for this study are based on the fundamental scientific objective of performing enhanced temperature and water vapor soundings for the European area. Other important scientific possibilities (e.g., vertical wind profiling via water vapor tracking within narrow vertical layers) will be considered, if they can be accomplished without complicating the instrument.

An important practical objective is to make the instrument as simple, reliable, and inexpensive as possible, but at the same time maintain in-orbit operational flexibility. Therefore, options which might provide substantial simplifications are sought for evaluation, in addition to performance enhancement options.

The general approach of this study is to define a baseline instrument from which options for operational and design variances can be evaluated using simulations of sounding performance. Temperature and water vapor sounding simulations will use the simultaneous retrieval technique developed for HIS aircraft data (Smith et al., 1989). Experimental verification of the simulation results will be achieved using existing HIS aircraft data coincident with ground truth observations (i.e. radiosondes) obtained during several field programs.

III. Results

A. Baseline Definition

The baseline design for the geosynchronous infrared sounder is a single Michelson interferometer with continuous and complete optical path difference (OPD) scanning. The maximum optical path length is assumed to be programmable. This allows the operational flexibility of choosing among high vertical resolution local area coverage, medium resolution regional area coverage, and global coverage at a lower vertical resolution. Adequate noise performance over a wide region (3.7 - 15 microns) of the infrared emission

spectrum is achieved by dividing the spectral coverage in three broad spectral bands (roughly, the 3.7-5 micron temperature sounding region, the 5-11 micron water band, and the 11-15 micron temperature sounding region). In addition, the design makes use of array detectors (3x3 cluster) to give parallel spatial sampling, thus increasing the spatial coverage rate by a factor of nine over a single field of view (FOV) instrument. Spectral mode definitions are given in Table I. A summary of the infrared sounder design parameters is given in Table II.

TABLE I. METEOSAT SOUNDER SPECTRAL RESOLUTION MODE DEFINITIONS

MODE	BAND 1	BAND 2	BAND 3
HIGH			
Max. OPD	$\pm 1.6 \text{ cm}^{-1}$	$\pm 0.7 \text{ cm}^{-1}$	$\pm 0.5 \text{ cm}^{-1}$
Resolution element	0.3 cm^{-1}	0.7 cm^{-1}	1.0 cm^{-1}
MEDIUM			
Max. OPD	$\pm 0.8 \text{ cm}^{-1}$	$\pm 0.35 \text{ cm}^{-1}$	$\pm 0.25 \text{ cm}^{-1}$
Resolution element	0.6 cm^{-1}	1.4 cm^{-1}	2.0 cm^{-1}
LOW			
Max. OPD	$\pm 0.16 \text{ cm}^{-1}$	$\pm 0.1 \text{ cm}^{-1}$	$\pm 0.1 \text{ cm}^{-1}$
Resolution element	3.1 cm^{-1}	5.0 cm^{-1}	5.0 cm^{-1}

TABLE II. METEOSAT INTERFEROMETER BASELINE DESIGN PARAMETERS

Type	Michelson plane mirror
Alignment	Dynamic auto-alignment
Maximum Mirror Travel	± 1.6 cm OPD (± 0.8 cm physical travel)
Mirror Travel by Mode	High Resolution ± 1.6 cm OPD Medium Resolution ± 0.8 cm OPD Low Resolution ± 0.16 cm OPD
Michelson Mirror Rate	4.0 cm OPD/sec
Beamsplitter	
Substrate	KBr or KCl
Coatings	Ge + Sb ₂ S ₃
Aperture Stop	Area 10.8 cm^2
Area x Solid angle	$4.45 \times 10^{-5} \text{ cm}^2\text{-sr}$
Cooling	Passive Radiative Cooler
Temperatures	
Fore Optics	290K
Interferometer	220K
Detectors	95K
Spectral Ranges	
Band 1	600 - 1100 cm^{-1}
Band 2	1100 - 1800 cm^{-1}
Band 3	2000 - 2700 cm^{-1}
Detectors	
Type	PC-HgCdTe in Bands 1 and 2 PV-HgCdTe in Band 3
Area	$2.3 \times 10^{-5} \text{ cm}^2$ in Bands 1 and 2 $5.8 \times 10^{-5} \text{ cm}^2$ in Band 3
D*	$3.7 \times 10^{10} \text{ cmHz}^{1/2}/\text{W}$ in Band 1 $9.0 \times 10^{10} \text{ cmHz}^{1/2}/\text{W}$ in Band 2 $1.2 \times 10^{12} \text{ cmHz}^{1/2}/\text{W}$ in Band 3
Optical Transmission	
Band 1	0.14
Band 2	0.11
Band 3	0.12
Simultaneous FOVs	9
FOV Diameter at Nadir	10 km
FOV Spacing	15 km in a 50km x 50km sounding region
Telescope Aperture	40 cm
Scan Capability	Full Earth and Space View
Step and Dwell Time	0.1sec, 0.5sec, and 1.0sec (by mode)
Visible Channels	One fixed detector per FOV
Radiometric Calibration	290K onboard Blackbody and Space View
Frequency of IR Cal	20 minutes or less
Spectrometer	Michelson plane mirror interferometer
Mass	< 150 kg
Power	< 150 W
Volume	comparable to Filter Instrument
Data Rate	1.5Mbits - 500kbits (Depending on data compression)
Coverage Rate	3000km x 3000km in 1 hour Mesoscale Mode 6000km x 3000km in 1 hour Regional Mode 12000km x 12000km in 1 hour Global Mode

B. Simulated Temperature and H₂O Sounding Performance

Conclusion

In this section, the relationships among spectral resolution, noise equivalent temperature, dwell time, and retrieval error of temperature and water vapor will be explored. The principal conclusions are contained in Figs. 1a-c for temperature, water vapor, and vertical resolution respectively, which show both the advantage of the interferometer design over that of a filter radiometer and the ability of the interferometer to achieve the sounding performance required to have a positive impact on forecast models.

Comparison with a Filter Radiometer

Figure 1a shows the root-mean-square (rms) temperature retrieval error at standard "mandatory" pressure levels obtainable with the GOES I filter radiometer compared with the temperature retrieval error expected from the baseline High spectral resolution Interferometer Sounder (HIS). Similarly, Fig. 1b shows the fractional error of retrieved precipitable water and Fig. 1c shows the vertical resolution of temperature, using the concept of Backus and Gilbert, 1970, and Rogers, 1986, for the same instruments. The curve labeled "GLOBAL HIS" corresponds to the baseline interferometer low resolution mode ($3\text{-}4\text{cm}^{-1}$) which has the same dwell time as the filter radiometer and hence, similar area coverage capabilities. The dramatic improvement of the low resolution interferometric data over the individual channels of the filter radiometer is evidence of the importance of the continuous nature of the spectra obtained naturally with the interferometer. Also shown in Figs. 1a-c (labelled "MESOSCALE HIS") is the additional improvement in sounding accuracy obtainable from the same baseline instrument when operated in high resolution mode. This mode is best suited for the study of the precursors to local severe weather both because of the high vertical resolution provided and because the additional dwell time required in the mode reduces the area coverage rate.

Spectral Resolution Dependence

One of the important tradeoffs in infrared temperature sounding from space is retrieval performance versus spectral resolution. Figures 2a-c demonstrate this relationship for temperature, water vapor, and vertical resolution by showing the simulated retrieval performance for each of the baseline spectral resolution modes. "HIGH" refers to high resolution mode, "MEDIUM" refers to medium resolution mode, and "LOW" refers to low resolution mode. See Table I for mode definitions. Figures 2a-c are a comparison of retrieval performance assuming the same spectral noise, NEdT, for each resolution. Under this assumption, the benefit of higher spectral resolution is clear, with higher spectral resolution there are more channels of data in each spectral band, useful for noise reduction, and the individual channels are "clearer", that is, there is less smearing of line centers into line wings and hence improved ability to discriminate upper level from lower level radiative contributions. For instance, Fig. 2c shows that, with a spectral noise of 0.25°C , the high resolution mode has a vertical resolution of about 1.2km at the 800mb level whereas in low resolution mode the vertical resolution has degraded to 1.8km while the medium resolution mode is intermediate between the two. While this analysis is correct for equal noise,

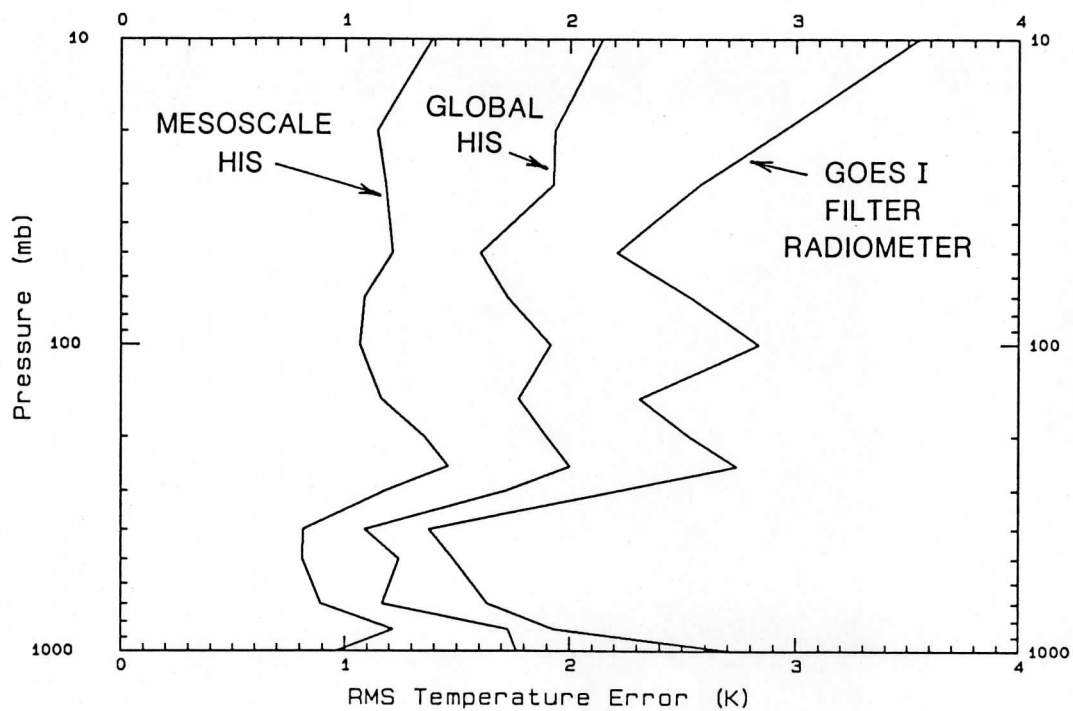


Figure 1a. RMS Temperature improvement of METEOSAT interferometer sounder over filter radiometer.

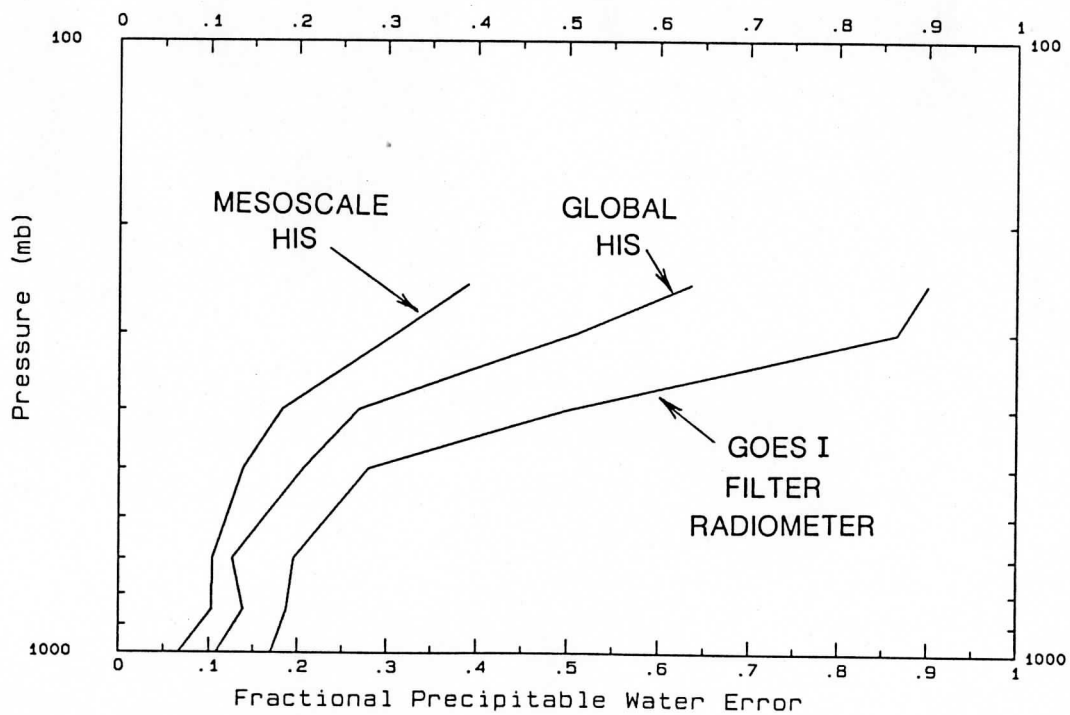


Figure 1b. Fractional Precipitable Water improvement of METEOSAT interferometer sounder over filter radiometer.

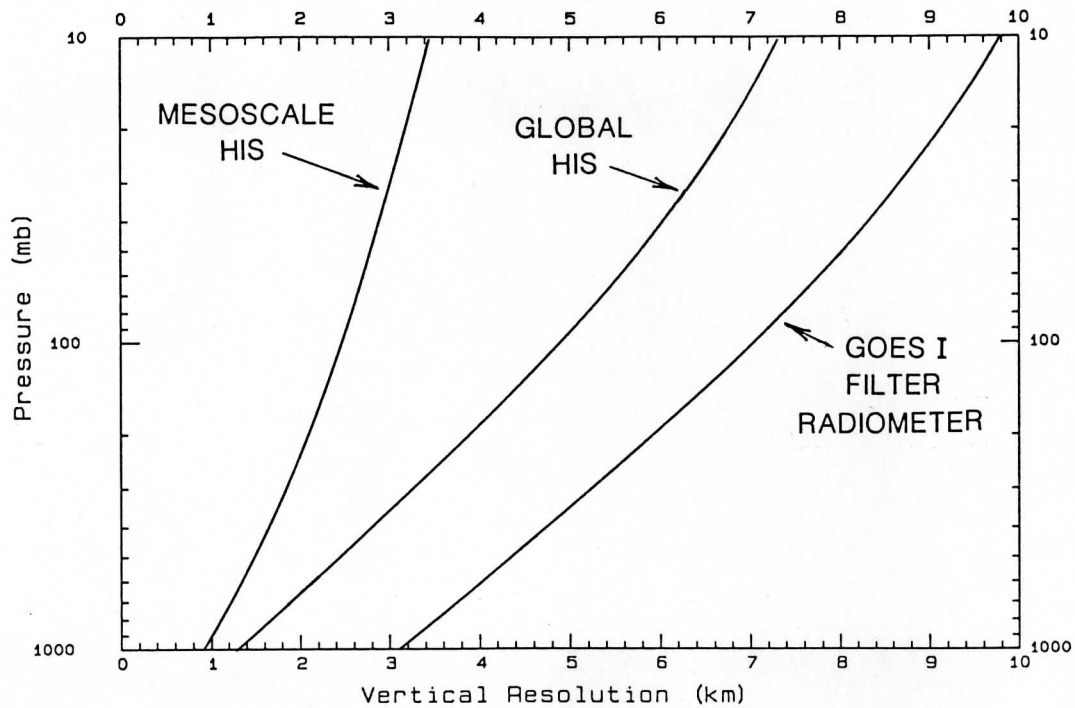


Figure 1c. Temperature Vertical Resolution improvement of METEOSAT interferometer sounder over filter radiometer.

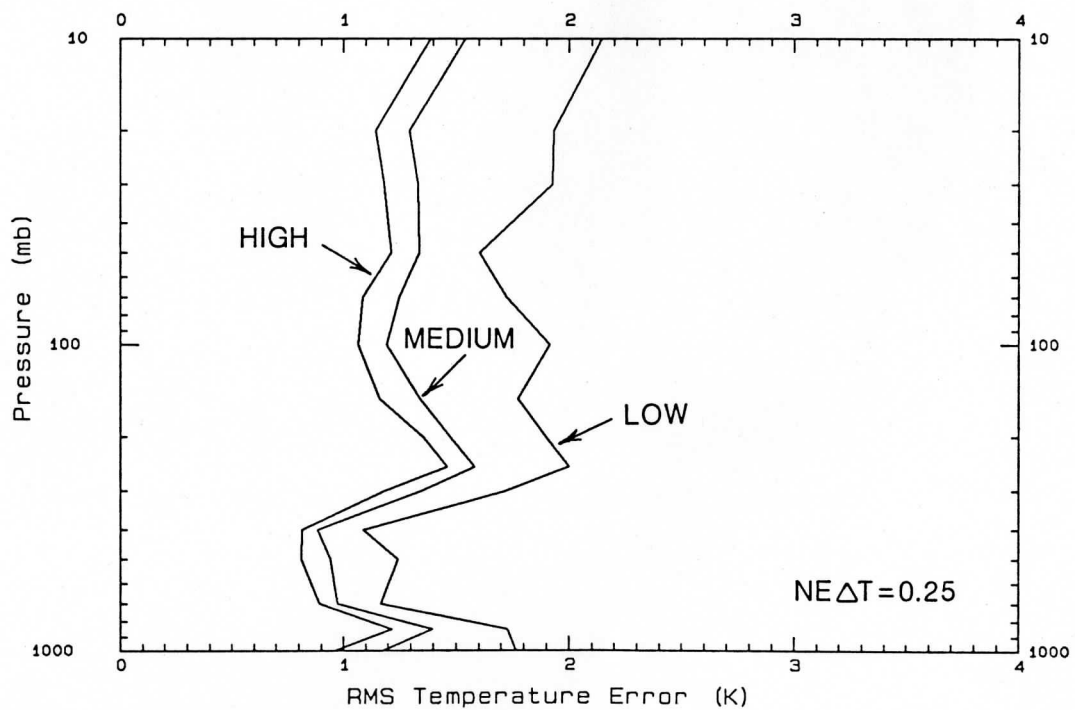


Figure 2a. Spectral Resolution dependence of RMS Temperature for METEOSAT interferometer sounder.

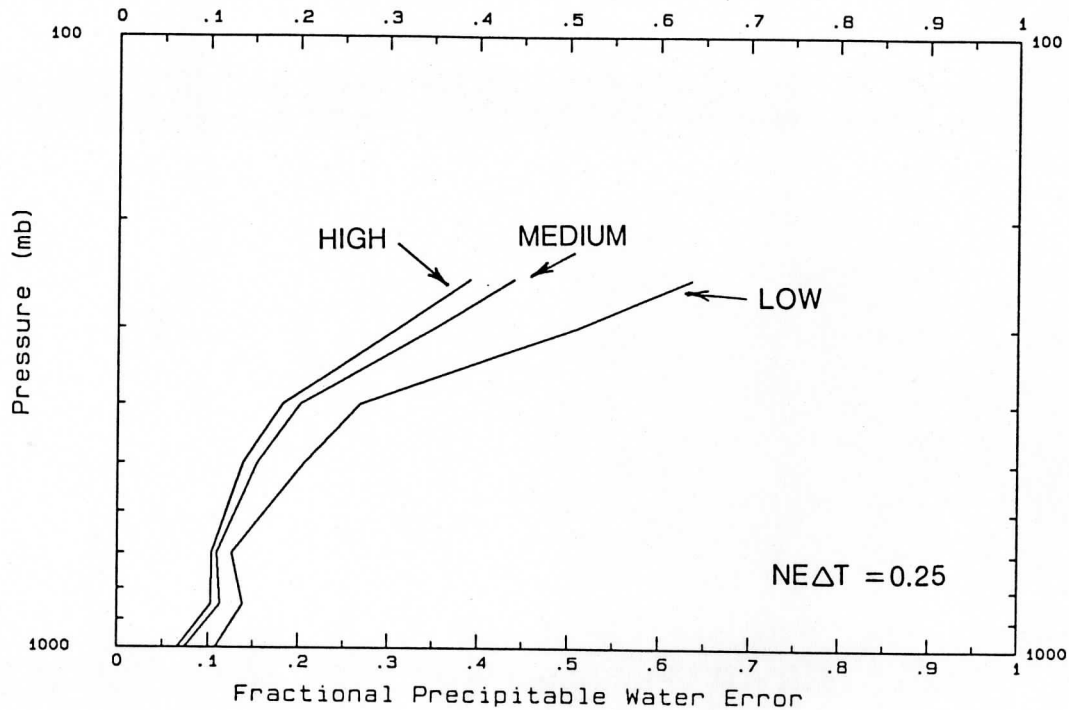


Figure 2b. Spectral Resolution dependence of RMS Precipitable Water for METEOSAT interferometer sounder.

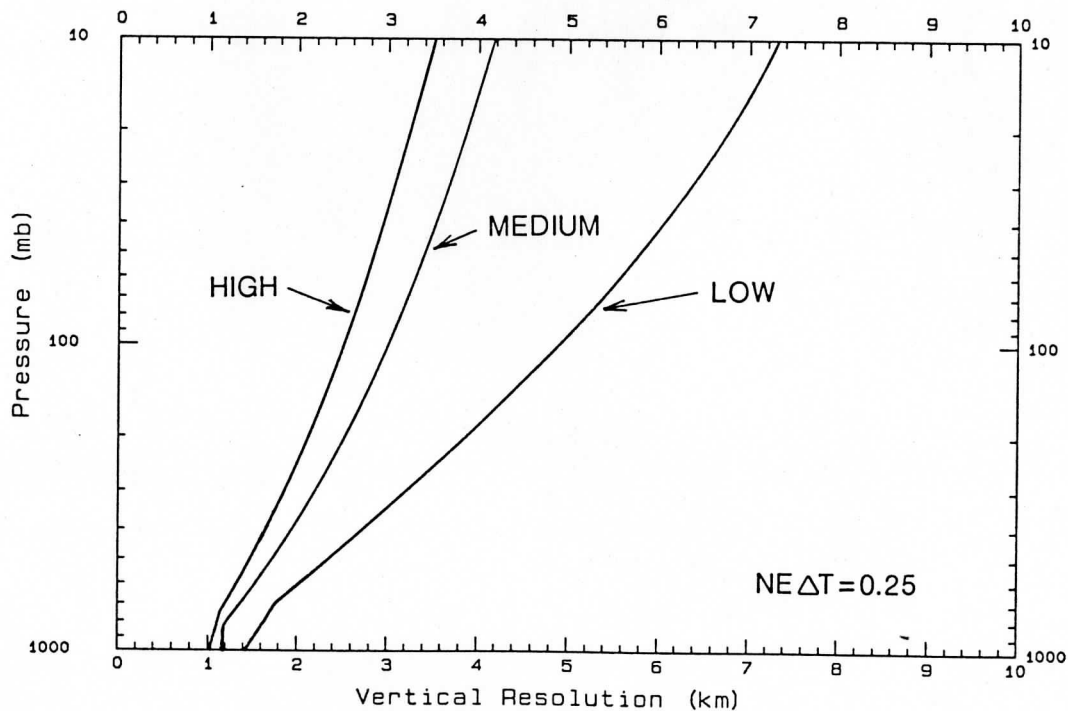


Figure 2c. Spectral Resolution dependence of Temperature Vertical Resolution for METEOSAT sounder.

the fact is that in normal operation the three operating modes will likely each have different noise levels associated with them. This leads us to an analysis of the dependence of the retrieval on spectral noise.

Spectral Noise Dependence

Another tradeoff in the instrument design important to retrieval performance is the dependence of spectral noise on retrieval accuracy. Figures 3a-c show, with medium resolution as an example, the dependence of varying spectral noise (NEdT) on the retrieval of temperature, water vapor and vertical resolution. As shown in, for instance, Fig. 3a, a reduction of the spectral noise (NEdT) causes a steady improvement in the retrieval accuracy (reduction of NEdT from 1.0°C to 0.125°C at the 700mb level reduces the rms temperature retrieval error from 1.3°C to 0.8°C in medium resolution mode). The same improvement is evident in precipitable water retrieval, Fig. 3b, and in vertical resolution, Fig. 3c.

For the purposes of this study, detailed simulations of temperature and water vapor retrieval error and of vertical resolution have been computed for each of the baseline modes (high, medium, and low; see Table I) at specific spectral noise (NEdT) levels. A layer average of rms retrieval errors was computed in order to characterize two important regions of the atmosphere. A 700-1000mb layer average was computed to demonstrate retrieval accuracy for both temperature and water vapor in the lower troposphere. A 200-300mb layer average was also computed for rms temperature retrieval error as a "worst case" example. In order to parameterize the spectral noise (NEdT) dependence of the retrievals, the temperature and fractional precipitable water retrieval errors have been fit to an analytical function of the form

$$F(\sigma) = a (1 - \exp [-\sigma/c]) + b \sigma + d \quad (1)$$

where σ is the spectral noise level (NEdT) in degrees Celsius, F is the function to be fit (either rms temperature error, or fractional precipitable water error), and a, b, c, and d are constants adjusted to obtain a best fit. All the resolution modes were fit well by this empirical function. The advantage of this analytic form is that a transformation of variables into dwell time and subsequent comparison of various operating modes is greatly simplified.

Characterization of the Noise

In order to compare the various operating modes fairly, spectral noise (NEdT) expected in each operating mode has been characterized as a function of dwell time. For an interferometer with constant OPD mirror velocity the relationship for detector noise [one component of spectral noise (NEdT)] is

$$NEN = \frac{\sqrt{[A_d]} * X * \sqrt{(2)} * 10^7}{A_0 * \Omega * t_0 * D^* * \sqrt{[1/(2*T_i)]}} \left[\frac{mW}{m^2 \text{ sr cm}^{-1}} \right] \quad (2)$$

where A_d = The area of the detector [cm^2]
 T_i = The integration time per scene [sec]
 A_0 = The area of the optics aperture [cm^2]
 t_0 = The overall optical system transmission.

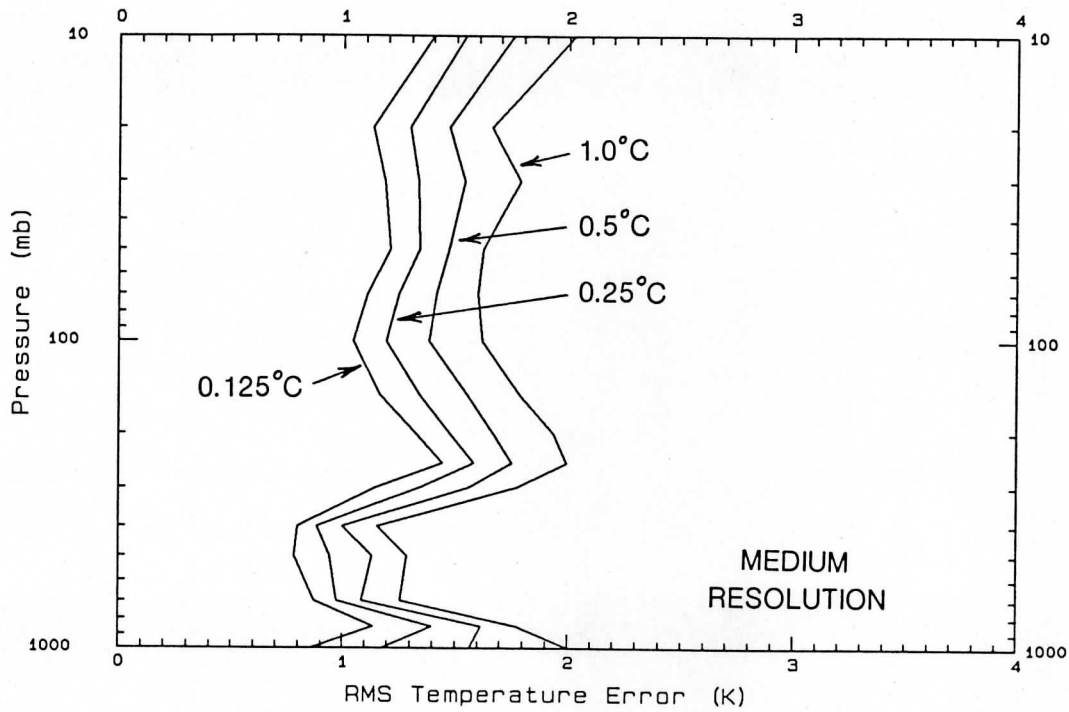


Figure 3a. METEOSAT sounder Spectral Noise (NEdT) dependence of RMS Temperature.

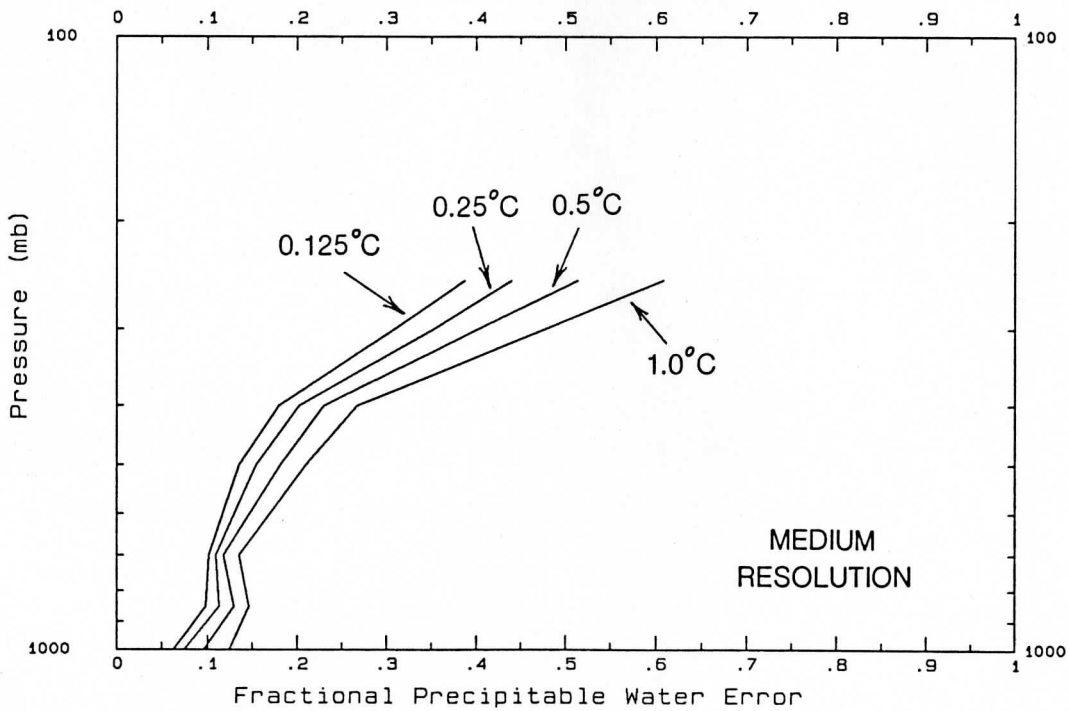


Figure 3b. METEOSAT sounder Spectral Noise (NEdT) dependence of RMS Precipitable Water.

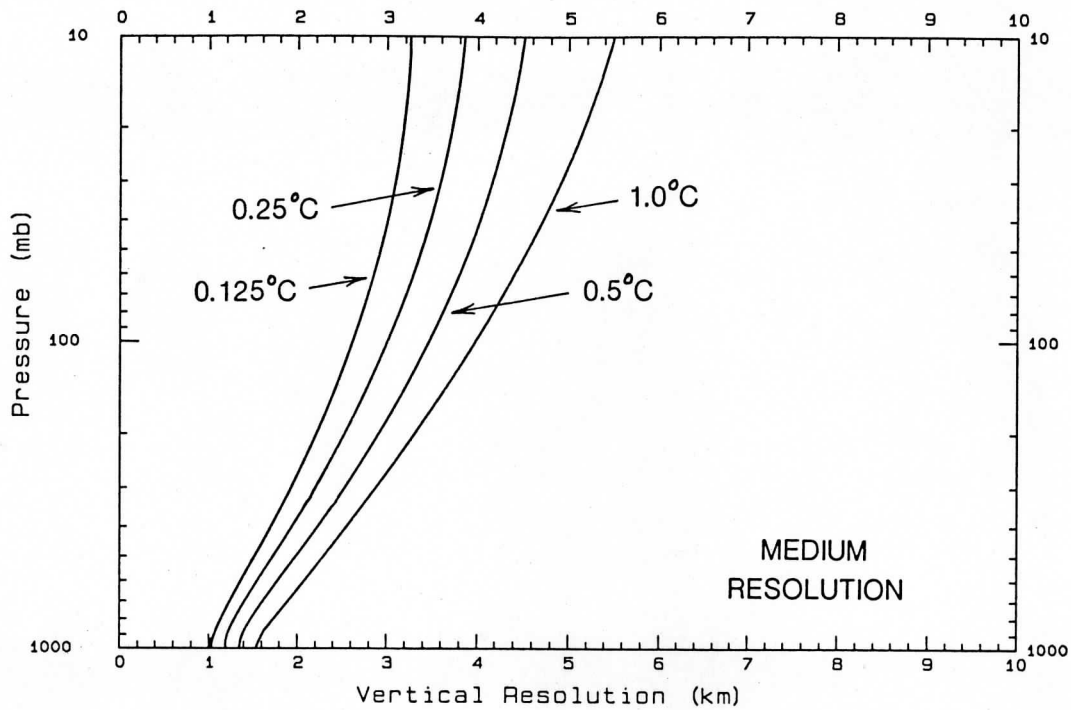


Figure 3c. METEOSAT sounder Spectral Noise (NEdT) dependence of Temperature Vertical Resolution.

Using the baseline parameters given in Table II, (see also NOAA Report: High-resolution Interferometer Modification of the GOES L/M Sounder: Feasibility Study) the values of the coefficients in this equation can be calculated and the proportionality constant between NEdT and dwell time can be computed. Note that this equation implies that, for a fixed dwell time, NEdT is directly proportional to maximum OPD travel (X). Thus one would expect that for a fixed dwell time that medium resolution mode would have an NEdT one half that of high resolution mode, and moreover, low resolution mode would have an NEdT one fifth that of medium. That this is true can be seen from a plot of NEdT detector noise versus dwell time shown in Fig. 4a for each of the operating modes; high, medium, and low (see Table I). However, in the real world, there are sources of noise beyond detector noise that also influence the ability of a retrieval algorithm to retrieve to generate accurate retrievals. Some of these sources may be instrumental, some may be atmospheric (clouds, haze, inversions, turbulence), some may be due to uncertainties in the molecular spectroscopy, and some may be due to numerical quadrature errors. All such errors that are both independent of the length of time spent dwelling in one spot and independent of spectral resolution will be referred to as "fixed" noise in the remainder of this report. A simple, but more realistic, parameterization of NEdT is presented below

$$\text{NEdT}(t)^2 = \text{Detector Noise}(t)^2 + (\text{"Fixed" Noise})^2 \quad (3)$$

where Detector Noise(t) refers to the equation for NEN above. This relation is illustrated in Fig. 4b for a fixed noise level of 0.1°C. The value of 0.1°C is thought to be a reasonably typical value given the current understanding of noise sources. In any actual case the fixed noise level may be greater or less.

Retrieval Versus Dwell Time

The comparison of retrieval errors versus dwell time is shown in Figs. 5, 6 and 7. Figure 5a shows the dependence of rms temperature error (Fig. 5b shows the fractional precipitable water error) versus dwell time for the various modes of an ideal sounder with no fixed noise. In general, these curves show that, with an ideal sounder, low resolution mode gives better performance than high resolution for short dwell times and comparable performance at longer dwell times. However, in the more realistic case shown in Figs. 6a and 6b we see that, with non-zero fixed noise, medium and high resolution modes consistently outperform the low resolution mode. The same conclusions follow from consideration of the 200-300mb "worst case" example shown in Figs. 7a and 7b.

C. Operational Scenarios

The baseline instrument, as conceived, has considerable in-orbit operational flexibility. It has three spectral resolution modes with minimum dwell time in each mode of 0.1 sec (low), 0.5 sec (medium), and 1.0 sec (high). (See Table I.) During these dwell times a 50 km at nadir square area is sampled with nine fields of view. Thus a 12,000 x 12,000 km area encompassing the earth disk can be covered in four hours in low resolution mode while a 3000 x 3000 "dense" sounding region can be covered in one hour using high resolution mode. In order to further reduce area coverage times

Noise vs Dwell Time

Fixed Noise = 0.0

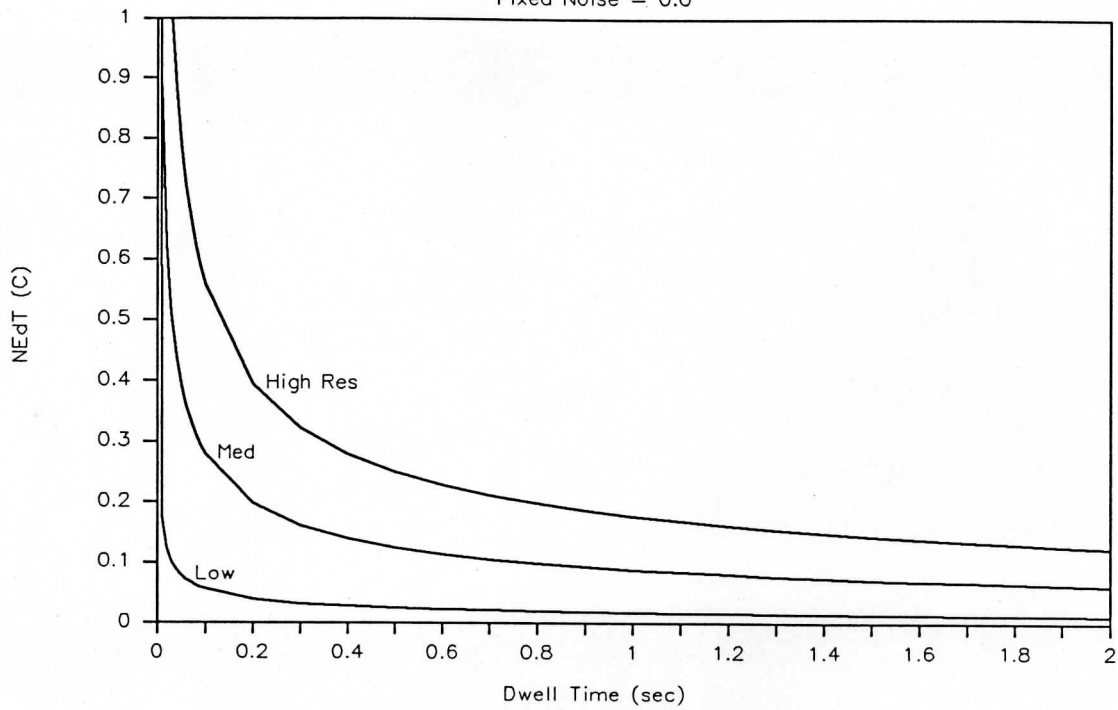


Figure 4a. Noise (NEdT) versus Dwell Time for zero fixed noise.

Noise vs Dwell Time

Fixed Noise = 0.1

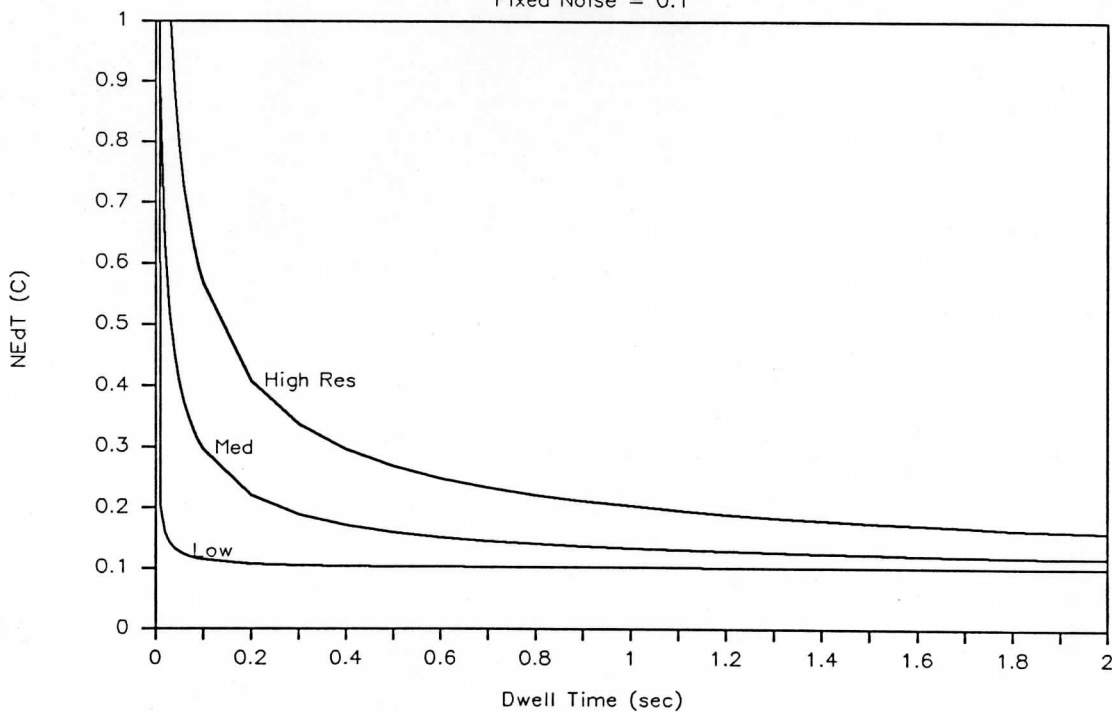


Figure 4b. Noise versus Dwell Time for nonzero fixed noise.

700-1000 mb Retrieval Errors (0.0 fn)

High=1.6,.77,.5cm;Med=/2;Low=/10

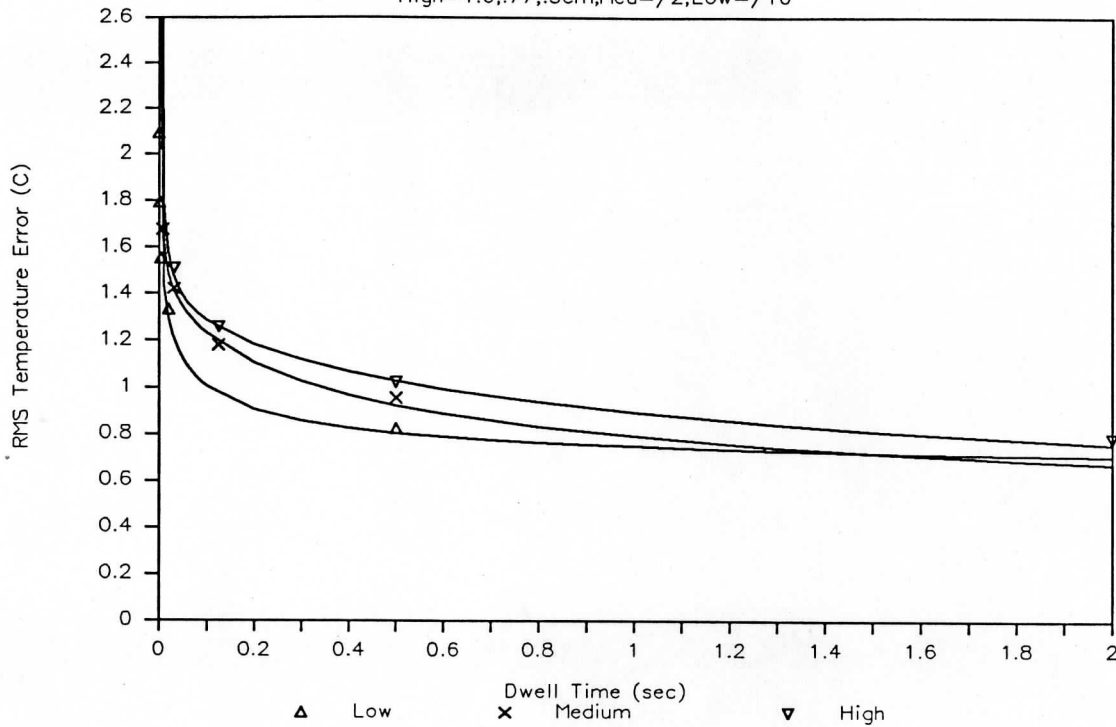


Figure 5a. RMS Temperature Retrieval Error without fixed noise for METEOSAT interferometer sounder.

700-1000 mb Retrieval Errors (0.0 fn)

High=1.6,.77,.5cm;Med=/2;Low=/10

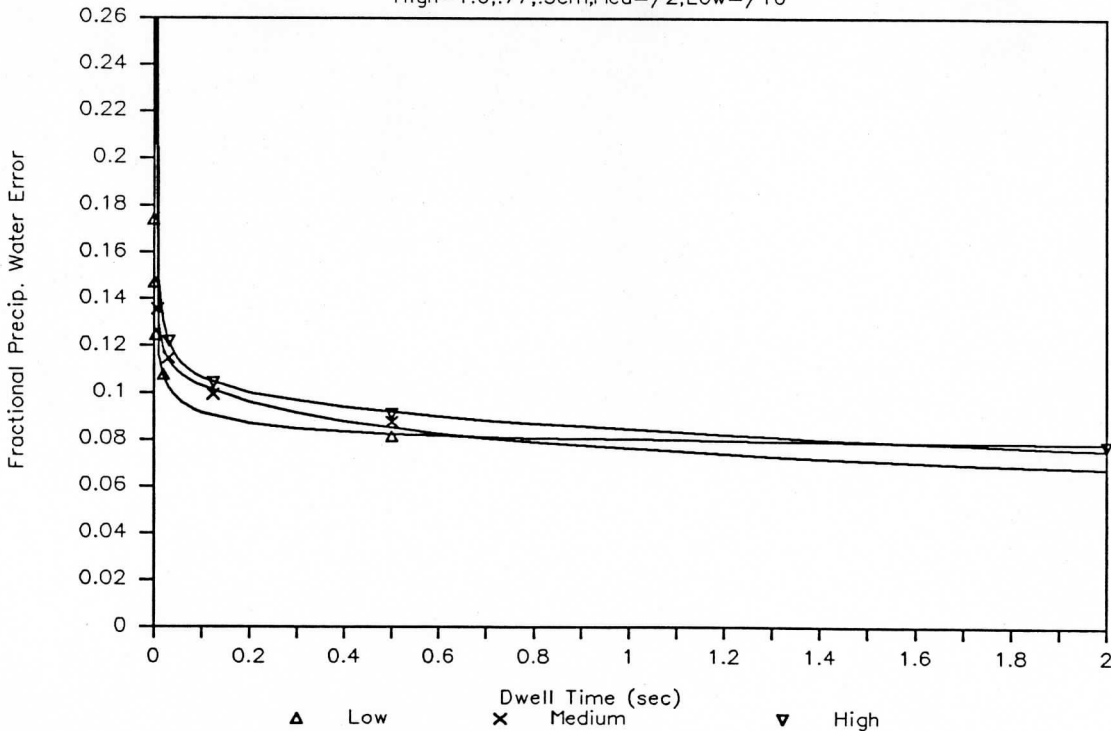


Figure 5b. RMS Precipitable Water Error without fixed noise.

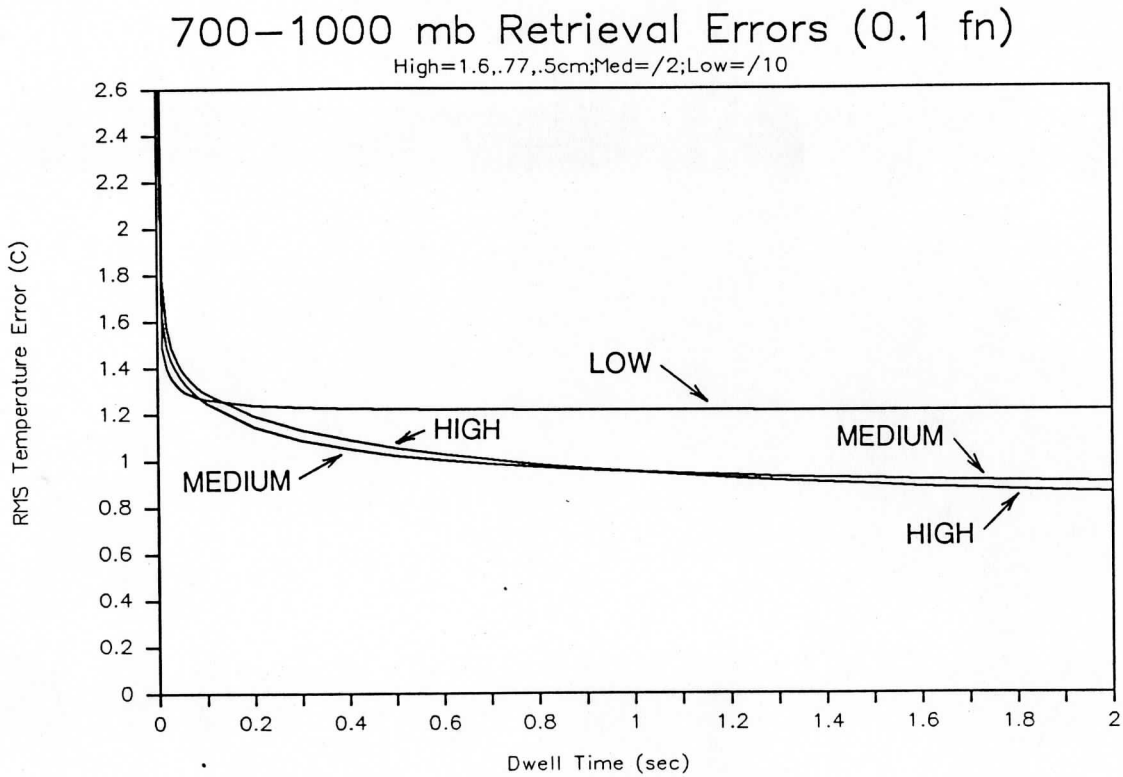


Figure 6a. RMS Temperature Retrieval Error with fixed noise.

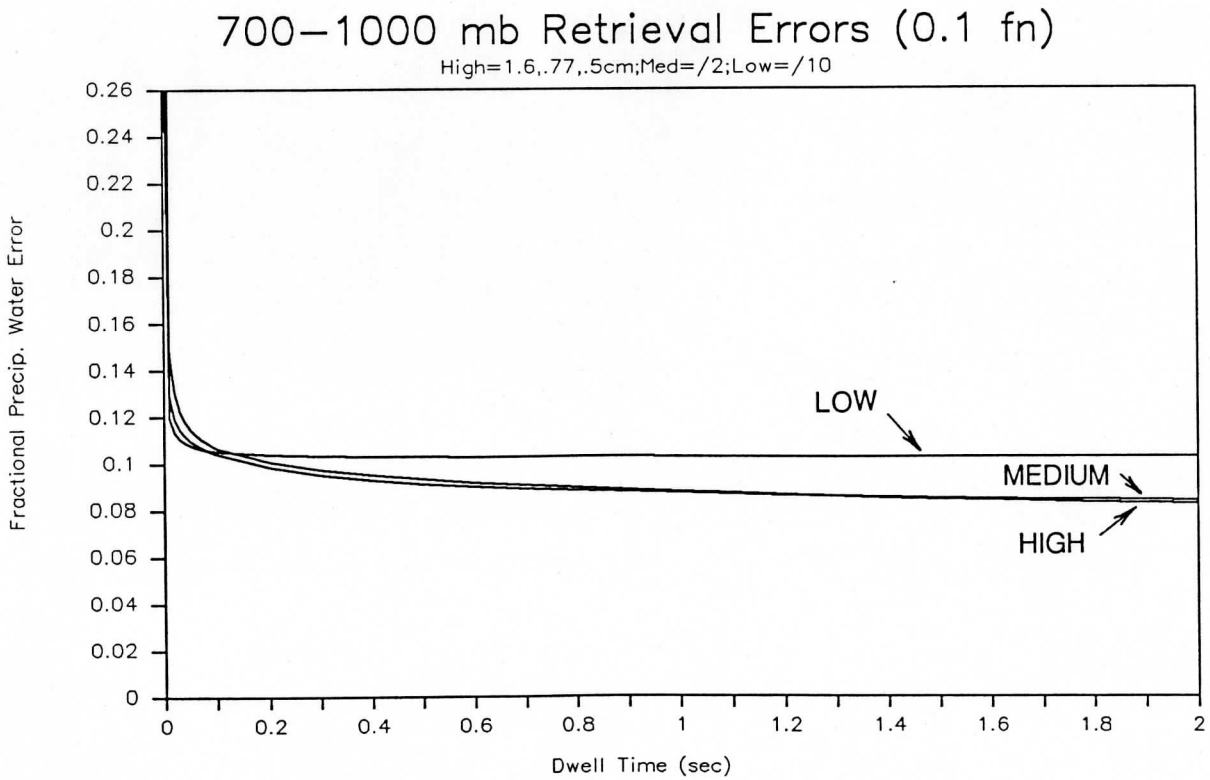


Figure 6b. RMS Precipitable Water Error with fixed noise.

200-300 mb Retrieval Errors (0.0 fn)

High=1.6,.77,.5cm;Med=/2;Low=/10

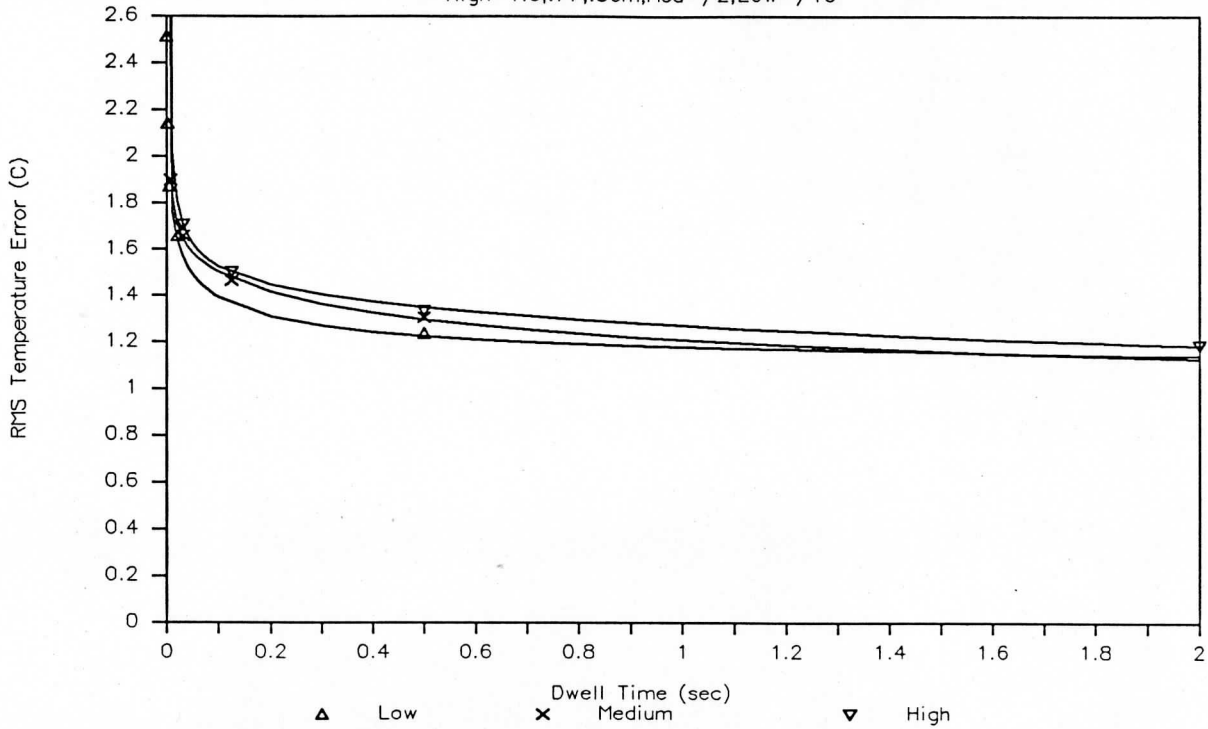


Figure 7a. RMS Temperature Retrieval Error without fixed noise.

200-300 mb Retrieval Errors (0.1 fn)

High=1.6,.77,.5cm;Med=/2;Low=/10

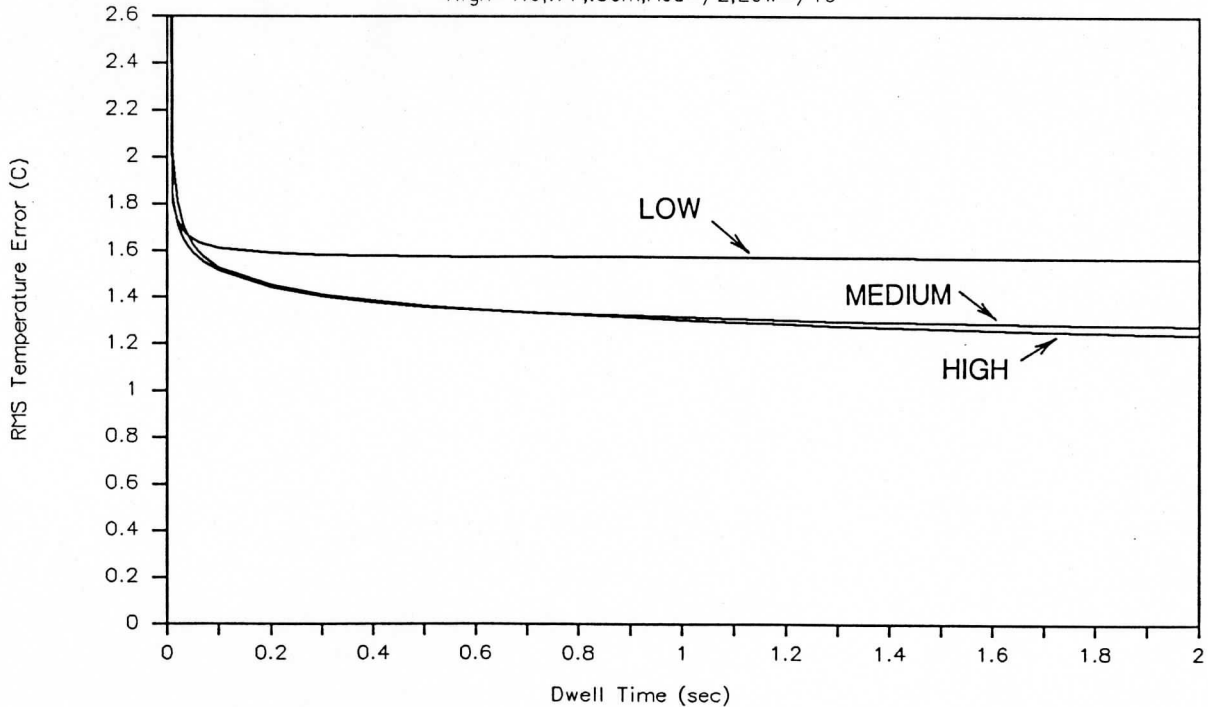


Figure 7b. RMS Temperature Retrieval Error with fixed noise.

one can make use of the step and dwell capability of the sounder telescope to sample 50 x 50 km square FOVs at intervals larger than 50 km. Table III gives an example of regional and global area coverage times using 50 km soundings spaced 100 and 150 km apart. Using 150 km sampling a full disk image could be generated every half hour. The ability to select rectangular sounding regions of arbitrary size, and choose among the possible vertical resolution modes and spatial sampling strategies allows the greatest operational flexibility to meet the changing needs of the meteorological application.

TABLE III. COVERAGE RATES

CLUSTER SEPARATION		DWELL TIME		
		1 sec High	1/2 sec Medium	1/4 sec Low
50 km	Regional	60 min	30 min	15 min
	Global	16 hrs	8 hrs	4 hrs
100 km	Regional	15 min	7.5 min	3.8 min
	Global	4 hrs	2 hrs	1 hrs
150 km	Regional	6.7 min	3.3 min	1.7 min
	Global	1.8 hrs	0.9 hrs	0.5 hrs

* Instantaneous Resolution is 10 km with a 15 km separation within each 3 x 3 field of view cluster.

[Region = 3000 x 3000 km]
 [Global = 12000 x 12000 km]

D. Variations from the Baseline

1. Enhancements

A method for optimal sampling of the interferometric temperature and water vapor data has been identified and the advantages and disadvantages of that design will be considered as a part of the final report. The possibility exists with this approach of combining the high vertical resolution from the high spectral resolution mode of the baseline with the rapid spatial coverage currently found in the low spectral resolution mode. This advantage comes at the additional complexity of two detector arrays besides the three already in the baseline design. Further analysis will be required to show whether or not this approach has a real performance advantage over the baseline design.

2. *Simplifications*

- reduce array dimensions to 2x2
- drop down to two spectral resolution modes

(To be determined)

E. Typical NEdT

Mean spectra and NEdT for given NEN in the following cases

- Tropical, Mid-latitude, Subarctic

(To be determined)

F. Documentation of Calibration Requirements

(To be determined)

G. Data Compression Techniques

(To be determined)

IV. *Summary*

In summary, there are three points that can be made; (1) a low resolution interferometer gives a substantial performance improvement over a filter wheel radiometer and has similar area coverage capabilities, (2) given the same dwell time both the medium and high resolution modes have a significant performance improvement over that of low resolution mode, and (3) the higher spectral resolution modes have the greatest vertical resolving capability. One can see that the METEOSAT baseline interferometer is an attractive instrument for achieving the sounding performance while maintaining the spatial coverage capabilities of existing systems through its low resolution mode.